Supporting Information

Hierarchical BiOCl flowerlike microspheres by room-temperature solid-state chemical reaction as a new anode for rechargeable magnesium ion batteries

Caixia Zhu[a], Yakun Tang[a], Lang Liu[a]*, Xiang Bai[a], Youyuan Xu[a], Yana Nuli[b], Jiulin Wang[a]

[a]State Key Laboratory of Chemistry and Utilization of Carbon Based Energy Resources; College of Chemistry, Xinjiang University, Urumqi, 830046, Xinjiang, PR China.

[b]School of Chemistry and Chemical Engineering, Shanghai Electrochemical Energy Devices Research Center, Shanghai Jiao Tong University, Shanghai 200240, P. R. China.

*E-mail: liulang@xju.edu.cn

Experiment section

1.1 Material characterizations

Bruker D8 X-ray diffraction (XRD) equipped with a diffractometer of Cu-Kα radiation was applied to test phase composition. The content of surfactant in the composites was estimated by thermogravimetric analysis (TGA, Discovery SDT 650) at a heating rate of 10 ^{o}C min^{-1} in O_2. Bruker VERTEX 70 spectrometer was used to record Fourier transform infrared spectra (FTIR). Nitrogen adsorption-desorption isotherms were obtained by ASAP 2460 equipment (Micromeritics Instruments, Xtended Pressure Sorption Analyzer). Specific surface areas of the samples were calculated by using the Brunauer-Emmett-Teller (BET) method, and pore size distributions were computed by using the Density Functional Theory (DFT) method.

The surface morphology of samples was characterized by scanning electron microscopy (SEM, Hitachi S-4800), transmission electron microscopy (TEM, Hitachi H-600) and high-resolution transmission electron microscopy (HRTEM). X-ray photoelectron spectrometry (XPS) test was performed using Thermo ESCALAB 250 mount with a monochromated Al X-ray resource to detect the valence state of elements in the samples. For ex-situ XPS and XRD analysis, the BiOCl electrode after discharging/charging to different states was taken out from the cell and washed thoroughly by tetrahydrofuran (THF).

1.2 Electrochemical measurements

BiOX, super P and polyvinylidene fluoride with a mass ratio of 8:1:1 were added into N-methyl-2-pyrrolidone to form a thick liquid. Then, the thick liquid is coated on a stainless steel foil and dried at 110 ^{o}C under vacuum for 12 h to obtain the electrode. Coin half-batteries were assembled in an argon-filled glove box by using magnesium metal as a counter electrode, the prepared electrode as the anode, and 0.4 M APC (2PhMgCl-$AlCl_3$/THF) as the electrolyte. Cyclic voltammogram (CV) data and electrochemical impedance spectroscopy (EIS) were collected by using the electrochemical CHI660D workstation (Chenhua, China). Galvanostatic charge/discharge (GCD) tests were performed on Land (CT2001A, China) at room temperature. After 5 cycles activization at 20 mA g^{-1}, the GITT curves were obtained at the constant current pulse of 20 mA g^{-1} with pulse and relaxation periods of 10 and 30 min, respectively. Specific capacities were calculated based on the mass of the anode material, and the typical loading of the active material ranges from 0.7 to 0.9 mg cm^{-2}.

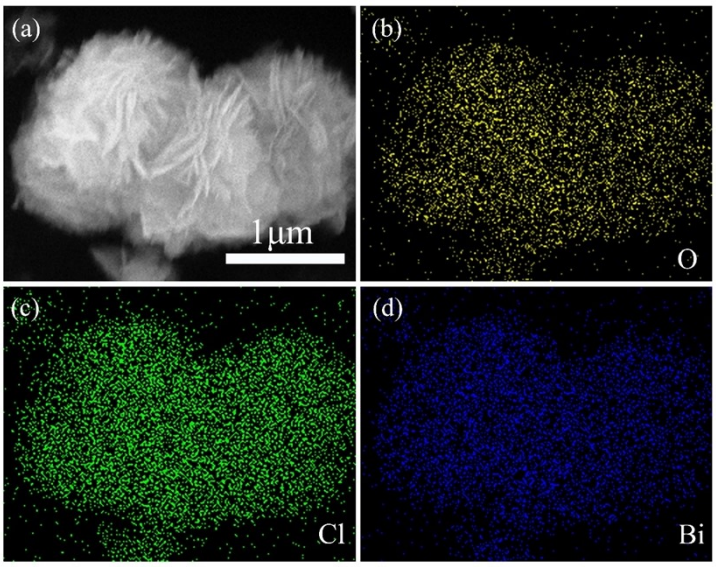

Figure S1 SEM (a) and corresponding EDS mapping images of oxygen (b), chlorine (c) and bismuth (d).

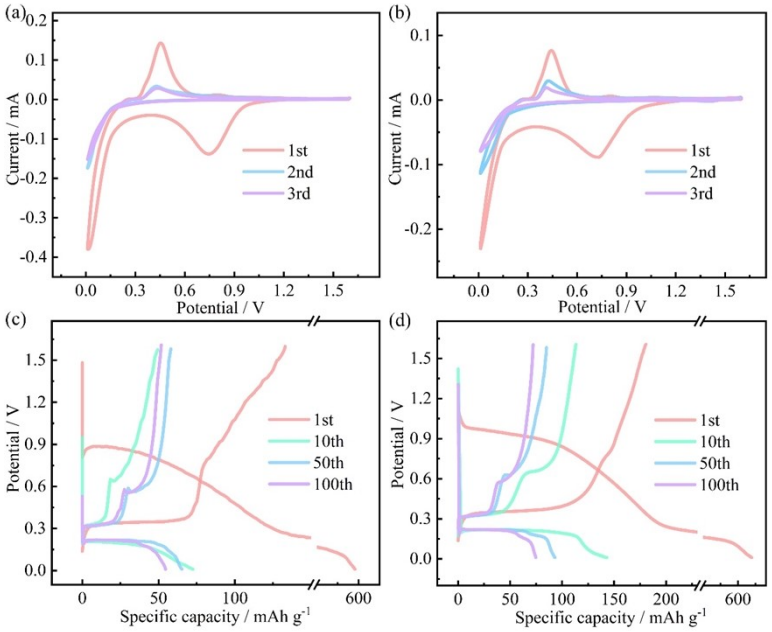

Figure S2 CV curves and GCD curves of BiOBr (a, c) and BiOI (b, d).

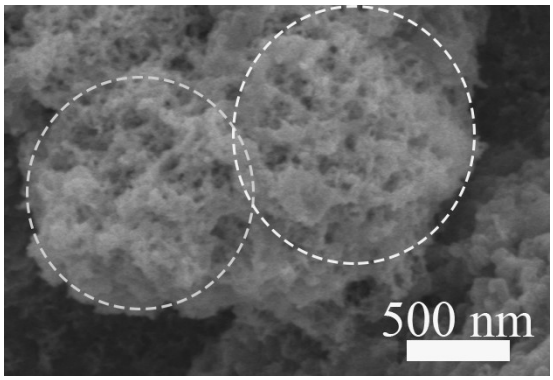

Figure S3 SEM image of the BiOCl electrode after 150 cycles at 50 mA g^{-1}.

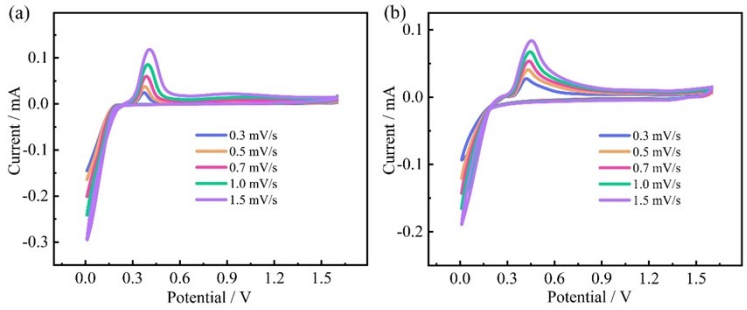

Figure S4 CV curves of BiOBr (a) and BiOI (b) at different scan rates.

The Mg^{2+} diffusion rate in the BiOX anode was evaluated by employing the CV test at different scan rates. The Mg^{2+} diffusion diffusivity (D_{Mg}) was obtained via the Randles-Sevchik equation [1]:

$$i_p=2.69\times10^5\times n^{3/2}\times S\times D_{Mg}{}^{1/2}\times C\times \upsilon^{1/2} \qquad (1)$$

Where i_p, n, S, C and υ are the peak current, the number of electrons, the surface area of the electrode, the concentration of Mg^{2+} ions and the scan rate, respectively.

The dynamics of Mg^{2+} diffusion in the BiOCl anode were evaluated by employing the galvanostatic intermittent titration technique. The Mg^{2+} diffusion diffusivity (D^{GITT}) was obtained via the following equation [2, 3]:

$$D^{GITT} = \frac{4}{\pi\tau}\left(\frac{m_B V_M}{M_B S}\right)^2\left(\frac{\Delta Es}{\Delta E\tau}\right)^2 \quad (2)$$

Where τ, m_B, V_M, and M_B are the constant current pulse duration, the mass loading, the molar volume, and the molar mass of the electrode material, respectively. S is the interface area between the electrode and the electrolyte. After a current pulse is conducted in a single-step GITT experiment, ΔE_s and ΔE_τ represent the changes in steady-state voltage and total cell voltage regardless of the IR drop, respectively. ΔE_s and ΔE_τ can be obtained from the GITT curves.

The electrochemical impedance spectra test was carried out to investigate the interface resistance of BiOX. The three samples are composed of semi-circles in the high-frequency region and straight lines in the low-frequency region. The semicircle in the high-frequency region is related to charge transfer resistance, while the straight line in the low-frequency region is related to magnesium ion diffusion in solid materials [4]. Obviously, BiOCl has the minimum transfer resistance, which means that the charge transfer at the solution/electrode interface is relatively easy.

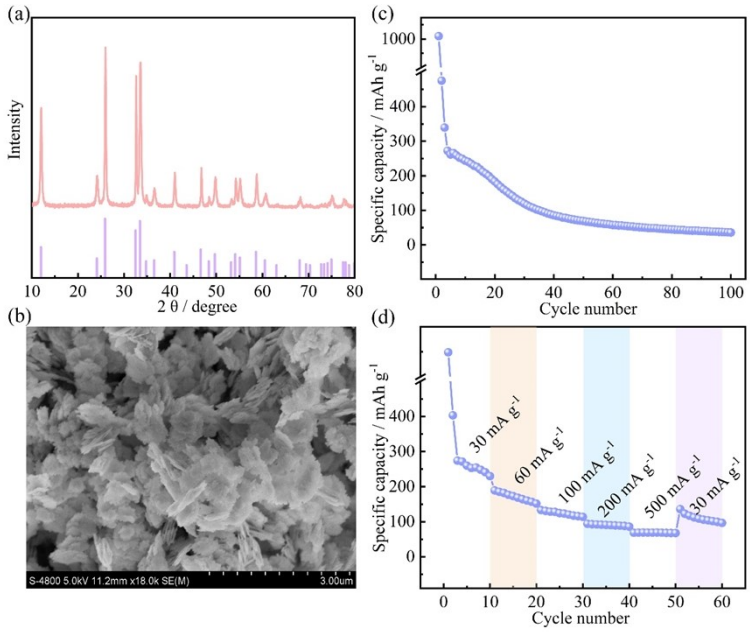

Figure S5 XRD patterns (a) and SEM image (b), cycling performances (c) and rate performances (d) of BiOCl nanosheets.

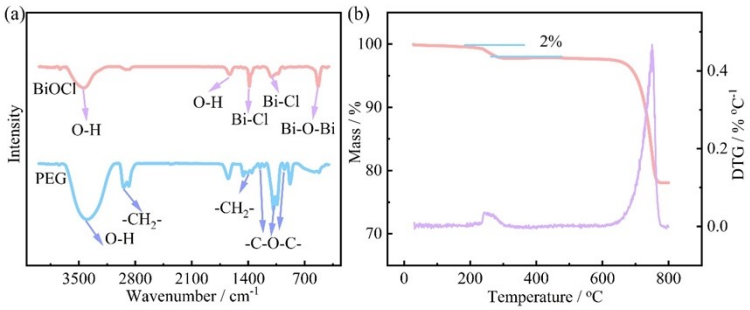

Figure S6 FTIR spectra of BiOCl and PEG (a), TG curves of BiOCl (b).

Infrared spectroscopy (FTIR) spectra exhibit that the absorption at about 520 cm^{-1} is ascribed to the stretching vibration of the Bi–O bond (Figure S4a). The symmetrical stretching vibration peak of Bi–Cl is reflected at 1380 cm^{-1} [5]. The stretching vibration and bending vibration peaks of O–H are reflected at 3440 and 1624 cm^{-1}, respectively. Besides, we also found weak PEG peaks [6] at 2877, 1460, 1250, 1094 and 948 cm^{-1} in the as-prepared samples, meaning that the sample contained a small amount of PEG (about 2%, Figure S4b).

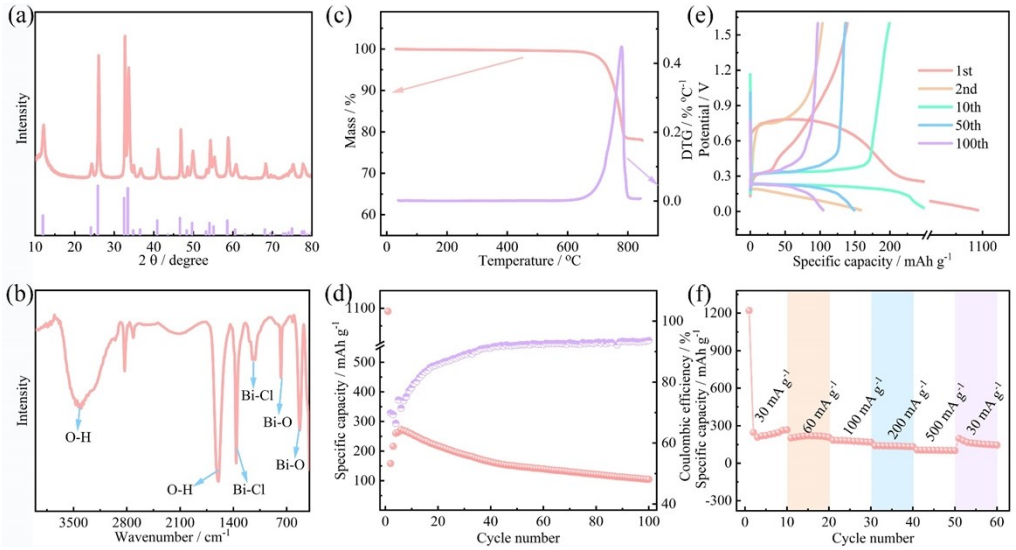

Figure S7 XRD patterns (a), IR spectrum (b), TG curve (c), cycle performances (d), CFD curves (e) and rate property (f) of BiOCl calcined at 350 °C.

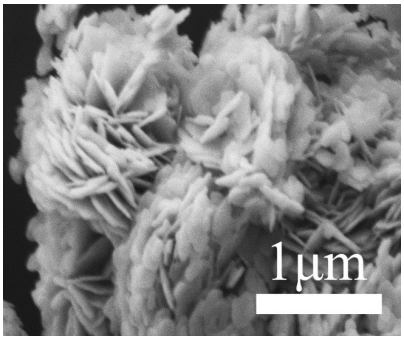

Figure S8 SEM image of BiOCl calcined at 350 °C.

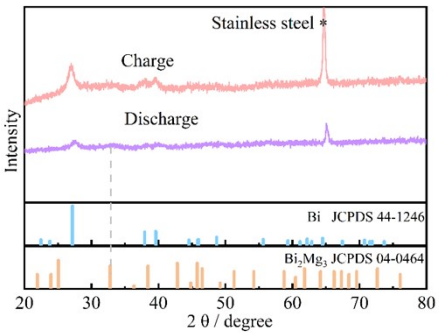

Figure S9 XRD patterns of the BiOCl electrode during the second cycle at different states.

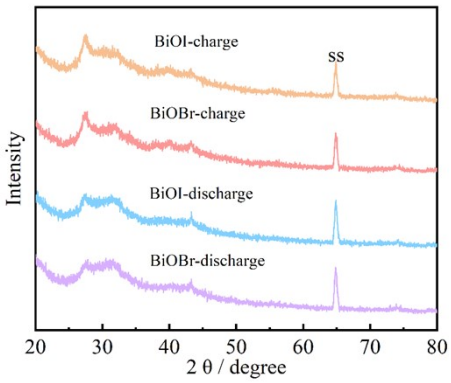

Figure S10 XRD patterns of the BiOBr/BiOI at different states.

Reference

1. M. Rastgoo Deylami, M. S. Chae and S. T. Hong, *Chem.Mater.*, 2018, **30**, 7464-7472.
2. W. Ren, F. Y. Xiong, Y. Q. Fan, Y. L. Xiong and Z. L. Jian, *ACS Appl. Mater. Interfaces*, 2020, **12**, 10471-10478.
3. Q. Y. An, Y. F. Li, D. H. Yoo, S. Chen, Q. Ru, L. Q. Mai and Y. Yao, *Nano Energy*, 2015, **18**, 265-272.
4. X. T. Lin, S. S. Qian, H. X. Yu, L. Yan, P. Li, Y. Y. Wu, N. B. Long, M. Shui and J. Shu, *ACS Sustainable Chem. Eng.* , 2016, **4**, 4859-4867.
5. J. Z. Wang, H. L. Li, X. R. Yan, C. Qian, Y. J. Xing, S. T. Yang, Z. K. Kang, J. Y. Han, W. X. Gu, H. Y. Yang and F. J. Xiao, *J. Alloy. Compd.*, 2019, **795**, 120-133.
6. Y. Zhou, R. Li, L. Tao, R. Li, X. Wang and P. Ning, *Fuel*, 2020, **268**, 117211.